American Journal of Energy Engineering
2026, Vol. 14, No. 3, pp. 151–157
https://doi.org/10.11648/j.ajee.20261403.16

SciencePG
Science Publishing Group

Research Article

Reversible Chlorine Storage in Li/Na-Cl_2 Batteries via the Open Framework of Fe-based Prussian Blue Analogue

Lina Ge[1], Yongpeng Cui[2], Wei Xing[1, *]

[1]School of Materials Science and Engineering, China University of Petroleum (East China), Qingdao, China

[2]College of New Energy and Materials, China University of Petroleum (Beijing), Beijing, China

Abstract

Rechargeable Li-Cl_2 and Na-Cl_2 batteries are regarded as promising high-energy-density energy-storage candidates owing to their appealing conversion electrochemistry between chlorine and alkali-metal chlorides. Nevertheless, practical deployment is greatly hindered by the shortage of reliable cathode host materials that can reversibly confine chlorine-related species and mitigate parasitic side reactions. Carbon materials and organic frameworks (MOFs/COFs) have been extensively investigated as chlorine hosts, whereas inorganic coordination host materials remain largely unexplored for metal-chlorine battery systems. Herein, we report an iron-based Prussian blue analogue (Fe-PBA) with an open monoclinic coordination framework as a new-type cathode host for both Na-Cl_2 and Li-Cl_2 batteries. Prepared via a facile coprecipitation route, Fe-PBA possesses interconnected 3D cavities that accommodate chlorine intermediates and facilitate ion transport. When applied in Na-Cl_2 batteries, Fe-PBA delivers stable cycling over 160 cycles, superior rate capability up to 3000 mA g^{-1}, and a large reversible capacity reaching 1434 mAh g^{-1}. Comparable electrochemical improvements are also realized in Li-Cl_2 configurations. Combined ex-situ EIS-DRT and XPS characterizations verify reversible Cl_2-chloride conversion within Fe-PBA cavities and confirm the structural robustness of the Fe-CN framework upon repeated cycling. This work expands the library of host materials for metal-chlorine batteries and demonstrates the great potential of inorganic Prussian-blue-analogue coordination frameworks toward high-performance chlorine-storage energy-storage devices.

Keywords

Prussian Blue Analogue, Li-Cl_2 Battery, Na-Cl_2 Battery, Reversible Chlorine Storage, Coordination Framework

1. Introduction

The increasing demand for high-energy-density electrochemical energy storage systems has stimulated the exploration of new battery chemistries beyond conventional lithium-ion batteries. Among various emerging technologies, rechargeable metal-chlorine batteries, particularly Li-Cl_2 and Na-Cl_2 systems, have attracted considerable attention owing to their high theoretical energy densities, abundant chlorine resources, and unique conversion-type electrochemical reactions. [1, 2] Unlike intercalation-based batteries, these systems rely on reversible conversion between chlorine species and metal chlorides. [3, 4] In typical liquid Li-Cl_2 and Na-Cl_2 bat-

*Correspondence: Wei Xing (xingwei@upc.edu.cn)

Received: 27 July 2026; **Accepted:** 28 August 2026; **Published:** 14 September 2026

Copyright: © The Author(s), 2026. Published by Science Publishing Group. This is an **Open Access** article, distributed under the terms of the Creative Commons Attribution 4.0 License (http://creativecommons.org/licenses/by/4.0/), which permits unrestricted use, distribution and reproduction in any medium, provided the original work is properly cited.

teries, $SOCl_2$-based chloroaluminate electrolytes enable chlorine redox chemistry, in which the initial discharge involves $SOCl_2$ reduction to generate LiCl/NaCl, followed by the reversible oxidation of metal chlorides to release Cl_2 during charging. [5, 6] Therefore, developing suitable cathode hosts capable of storing chlorine species and maintaining reversible Cl_2/chloride salts conversion is critical for advancing metal-chlorine batteries.

To date, porous carbon materials have been widely explored as chlorine hosts due to their high electrical conductivity, large surface areas, and accessible pore structures. [7, 8] In addition, porous organic frameworks, including covalent organic frameworks (COFs) [9] and metal-organic frameworks (MOFs) [5], have been investigated owing to their ordered pore architectures and structural tunability. These studies demonstrate the importance of host structures in regulating chlorine storage and conversion behavior. However, expanding chlorine host materials beyond conventional carbon and organic frameworks remains highly desirable for understanding the relationship between host structures and chlorine electrochemistry. Prussian blue analogues (PBAs) represent a class of inorganic coordination frameworks featuring three-dimensional open structures, adjustable metal centers, and interconnected channels. [10, 11] Their unique framework characteristics have enabled broad applications in electrochemical energy storage, ion sieving, catalysis, and molecular adsorption. In particular, iron-based Prussian blue consists of a stable Fe-CN coordination network, and the periodic arrangement of metal centers and cyanide bridges forms open cavities capable of accommodating guest molecules, potentially serving as an alternative host for chlorine storage. [12, 13] Moreover, the presence of coordinated metal sites and polar framework environments may provide additional interactions with reactive intermediates during electrochemical processes. However, their application in rechargeable metal-chlorine batteries has not been explored.

Herein, we introduce a sodium-containing iron-based Prussian blue analogue (Fe-PBA) coordination framework as a cathode host for Na-Cl_2 and Li-Cl_2 batteries. The Fe-PBA material was synthesized through a facile coprecipitation method, and exhibits a typical monoclinic phase with an open framework architecture. When employed as the cathode host, Fe-PBA enables reversible chlorine conversion in both Na-Cl_2 and Li-Cl_2 systems, delivering stable cycling performance, high-rate capability, and large reversible capacities. This work demonstrates the feasibility of coordination-based inorganic frameworks as chlorine hosts and provides a new material platform for the development of rechargeable metal-chlorine batteries.

2. Experimental Section

2.1. Preparation of Fe-PBA

In this experiment, all raw materials were purchased from Aladdin. Specifically, 4 mmol of $Na_4Fe(CN)_6 \cdot 10H_2O$ and 12 mmol of sodium citrate were dissolved in 100 mL deionized water to prepare solution A. Next, 4 mmol of $FeSO_4 \cdot 7H_2O$ and 12 mmol of sodium citrate were dissolved in 100 mL of deionized water to prepare solution B. After each of the above solutions was stirred for 1 h, solution B was dropped into solution A with the aid of a peristaltic pump at a dropping rate of 1 mL min^{-1}. Then the mixture was left to age for 12 h. The precipitate was obtained by centrifugation, during which it was washed several times with deionized water and ethanol. Finally, the moist precipitate was placed in a vacuum oven at 120 ℃ for 12 h to obtain Fe-PBA powder.

2.2. Material Characterizations

Morphology was analyzed using SEM (JEOL, JSM7900F). Raman spectroscopy measurements were performed using a Horiba HR Evolution with a 532 nm excitation wavelength. The crystal structure was characterized by XRD (Shimadzu, XRD-7000, Cu Kα radiation, λ = 1.542 Å). XPS measurements were performed using a Thermo Scientific K-Alpha.

2.3. Electrochemical Testing

The electrochemical tests were performed in CR2032 coin-type cells. The slurry was prepared by mixing the active material, the conductive agent (Super P), and the binder (poly(vinylidene fluoride)) at a mass ratio of 7:2:1 by weight and was dispersed in N-methyl-1,2-pyrrolidone solution for 12 h. The slurry was then coated on the stainless collector and dried overnight in a vacuum oven at 120 ℃. Sodium metal was used as the anode, and glass fiber from Whatman was used as the separator. The entire operation was carried out in a glove box filled with argon gas. Added 1 mmol of anhydrous $AlCl_3$ to 1 mL of $SOCl_2$ solution, then added 2 wt% NaFSI (LiFSI) and NaTFSI (LiTFSI) and stired for 20 minutes until dissolved to obtain the pristine electrolyte for the Na-Cl_2 (Li-Cl_2) battery.

Galvanostatic charge/discharge testing was performed using the LANHE CT3002A battery test system. At a specific current density, the charging step was controlled by setting the charge specific capacity, and the discharging step was controlled by setting the discharge cut-off voltage to 2 V. Ex-situ electrochemical impedance spectroscopy analysis was conducted on the electrochemical workstation (BioLogic) within a frequency range of 0.01 to 100 kHz.

3. Results and Discussion

Iron-based Prussian blue analogue (Fe-PBA) was synthesized via a room-temperature coprecipitation method with $Na_4[Fe(CN)_6]$, Fe^{2+} salts, and sodium citrate as precursors (Figure 1a). [14, 15] To improve the crystallinity of Fe-PBA, sodium citrate was used as a chelating agent to slowly release Fe^{2+} to control the reaction rate. As shown in Figure 1b, scanning

electron microscopy (SEM) images reveal that Fe-PBA exhibits well-defined cubic particles with micrometer-scale dimensions. Furthermore, the X-ray diffraction (XRD) pattern displays characteristic diffraction peaks located at approximately 17 °, 24 °, 34 °, 38 °, 48 °, and 55 °, corresponding to the (200), (220), (400), (420), (422), and (620) planes of the monoclinic phase structure, respectively (Figure 1c). No impurity peaks were detected, confirming the successful formation of pure-phase Fe-PBA. The structural formula for the monoclinic phase of Fe-PBA is typically $Na_xFe[Fe(CN)_6]$, where $1<X<2$. Additionally, the Raman spectrum exhibits three characteristic C≡N stretching vibrations at 2070, 2114, and 2137 cm^{-1} (Figure 1d). [15, 16] Specifically, the peak at 2137 cm^{-1} is assigned to Fe^{2+}-CN-Fe^{2+} coordination, while the bands around 2114 and 2070 cm^{-1} originate from mixed-valence $Fe^{2+/3+}$-CN environments, confirming the formation of the Fe-CN coordination framework. [17] This open three-dimensional framework structure of Fe-PBA provides a space for the storage of chlorine species, facilitating ion transport and electrolyte permeation.

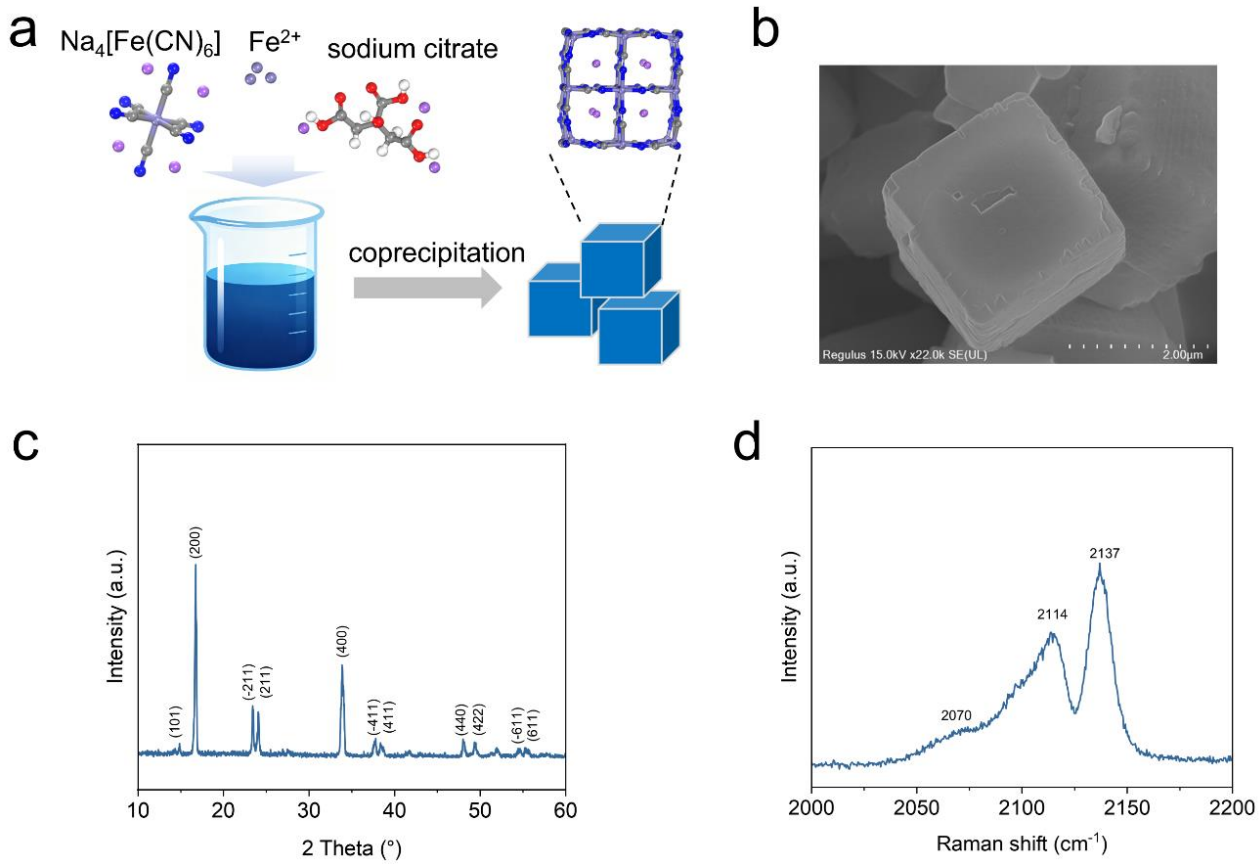

Figure 1. *(a) Schematic diagram of synthesis of Fe-PBA material; (b) SEM image, (c) XRD spectrum, and (d) Raman spectrum of the Fe-PBA material.*

The chlorine conversion capability of the Fe-PBA material was first evaluated in a Na-Cl_2 battery. As shown in Figure 2a, at a charge capacity of 500 mAh g^{-1}, the Fe-PBA material exhibited stable cycling performance over 160 cycles. Throughout the 160 cycles, the coulombic efficiency remained consistently close to 100%. This indicates that the Cl_2/NaCl conversion is highly reversible within the three-dimensional open framework of Fe-PBA. [5, 9] The charge-discharge curves for different cycles show stable voltage characteristics (Figure 2b). The rate performance was further evaluated under conditions where the charge capacity was controlled at 700 mAh g^{-1} (Figure 2c, d). As the current density was gradually increased from 150 mA g^{-1} to 3000 mA g^{-1}, the Fe-PBA cathode maintained a discharge capacity of approximately 700 mAh g^{-1}. When the current density was returned to 150 mA g^{-1}, the capacity rebounded to about 760 mAh g^{-1}, demonstrating rapid reaction kinetics. To further evaluate the maximum reversible capacity of the Fe-PBA cathode, charge-discharge tests were conducted by gradually increasing the charge capacity from 300 to 1,500 mAh g^{-1} (Figure 2e). Even at a charge capacity as high as 1,500 mAh g^{-1}, the battery maintained a reversible discharge capacity above 1,434 mAh g^{-1}, indicating that the chlorine species stored within the Fe-PBA framework achieve high conversion efficiency.

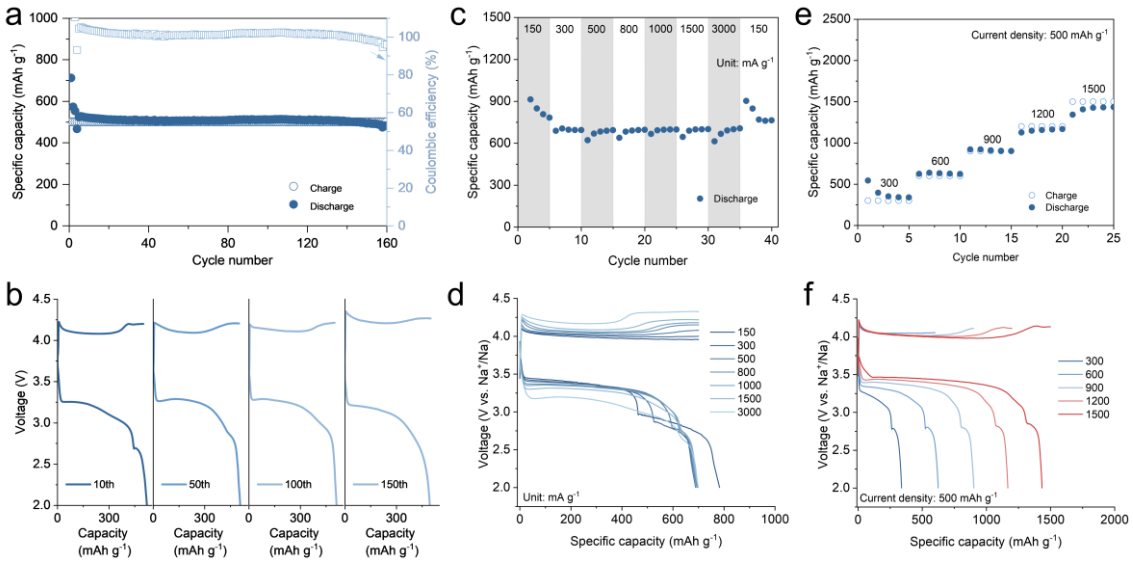

Figure 2. *Fe-PBA material for Na-Cl_2 batteries. (a) Cycling performance and (b) corresponding charge-discharge curves with a charging capacity of 500 mAh g^{-1} at 1 A g^{-1}; (c) Rate performance and (d) corresponding charge-discharge curves; (e) Extreme reversible capacity test under charge capacities of 300-1500 mAh g^{-1} at 0.5 A g^{-1}.*

To demonstrate the versatility of the Fe-PBA material for storing chlorine species, it was further applied as a cathode in a Li-Cl_2 battery. As shown in Figure 3a, the Fe-PBA cathode exhibited stable cycling performance at a fixed charge capacity of 500 mAh g^{-1}. After approximately 170 cycles, the discharge capacity remained at around 500 mAh g^{-1}, and the coulombic efficiency consistently stayed above 95%. The corresponding charge-discharge curves display a stable voltage plateau, confirming the reversibility of the LiCl/Cl_2 conversion process (Figure 3b). [18] Next, the rate performance of Fe-PBA was evaluated over a current density range of 150 to 3000 mA g^{-1} with a charging capacity of 700 mAh g^{-1} (Figure 3c, d). Notably, even at a high current density of 3000 mA g^{-1}, the electrode maintained a stable capacity of over 680 mAh g^{-1}. When the current density was reverted to 150 mA g^{-1}, the capacity recovered to 700 mAh g^{-1}, indicating that the Fe-PBA cathode also exhibits rapid chlorine conversion kinetics in Li-Cl_2 batteries. Additionally, the maximum reversible capacity test (Figure 3e) indicates that Fe-PBA can accommodate an increasing chlorine content. At a charge capacity of 1,500 mAh g^{-1}, the Fe-PBA cathode exhibited a reversible capacity of ~1,330 mAh g^{-1}, demonstrating the Fe-PBA framework's effective chlorine storage capability in the Li-Cl_2 battery.

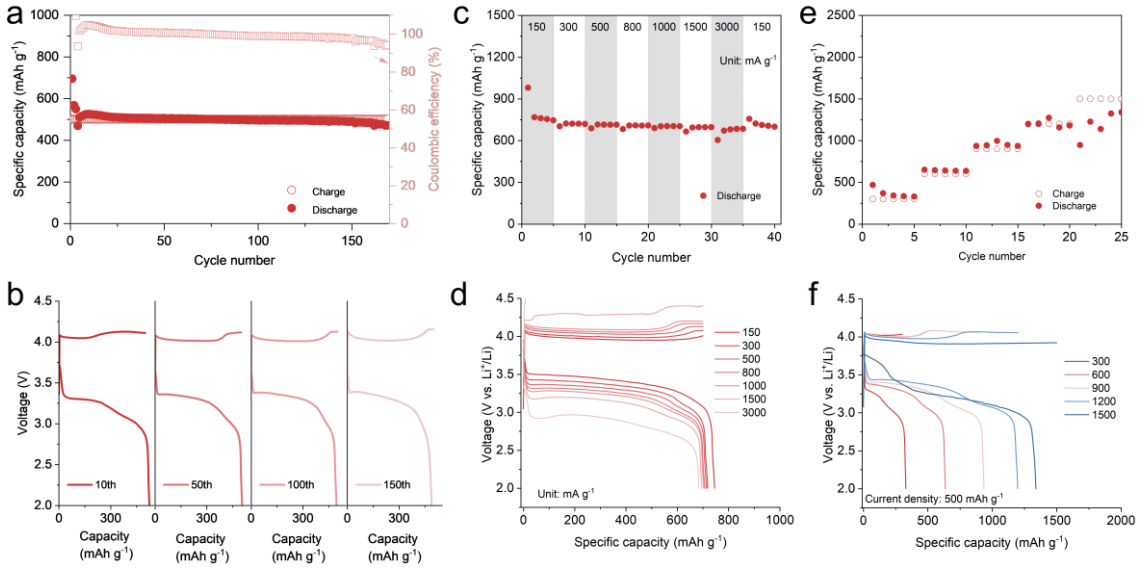

Figure 3. *Fe-PBA material for Li-Cl_2 batteries. (a) Cycling performance and (b) corresponding charge-discharge curves with a charging capacity of 500 mAh g^{-1} at 1 A g^{-1}; (c) Rate performance and (d) corresponding charge-discharge curves; (e) Extreme reversible capacity test under charge capacities of 300-1500 mAh g^{-1} at 0.5 A g^{-1}.*

To investigate the energy storage mechanism of the Fe-PBA cathode in alkali metal-chlorine batteries, ex-situ electrochemical impedance spectroscopy (EIS) and X-ray photoelectron spectroscopy (XPS) measurements were conducted as case studies using a Na-Cl_2 battery. The impedance spectra shown in Figure 4a, c reveal that the system's impedance exhibits significant changes during charge-discharge processes. Specifically, during discharge to 2 V, the impedance gradually increased, indicating that the insulating NaCl generated during discharge causes electrode passivation, which hindered charge transfer; however, as the charging process proceeds, the impedance gradually decreased throughout the process and is significantly lower than the discharge state, suggesting that the interfacial reaction kinetics improve effectively during the oxidation of NaCl to Cl_2. [19, 20] DRT results further reveal that the impedance contributions at different time scales primarily stem from interfacial charge transfer and ion diffusion processes. Notably, the charge transfer and ion diffusion impedances of the charged electrodes were significantly reduced, indicating that the Fe-PBA open framework facilitates the conversion of NaCl to Cl_2 (Figure 4b, d). [21] Furthermore, the surface chemical evolution during the cycling process was investigated via XPS measurements (Figure 4e). In the Cl 2p spectrum, the discharged state primarily exhibited a Na-Cl signal, while subsequent charging states displayed a significant increase in the Cl-Cl signal, indicating that the discharge product NaCl was consumed and converted into Cl_2, which was subsequently stored within the Fe-PBA open cavities. [6, 7] Meanwhile, the S 2p spectrum revealed the presence of sulfur oxide species associated with $Na_2SO_4/Na_2S_2O_3$, as well as S^0 species. During the first discharge cycle, $SOCl_2$ was reduced and decomposed into NaCl, S, and SO_2. After charging, $Na_2SO_4/Na_2S_2O_3$ remained present, while the contribution of S^0 decreased significantly, indicating that elemental S may have been consumed in a side reaction with Cl_2 during the charging stage. [1, 19] The Fe 2p XPS spectra indicate the presence of both Fe^{2+} and Fe^{3+} species in the Fe-PBA material both during discharge and charge, indicating that the Fe-CN framework remains stable during cycling. [14, 22] The slightly disordered Fe 2p spectrum observed in the discharged state may be attributed to the passivation of the electrode surface by NaCl products.

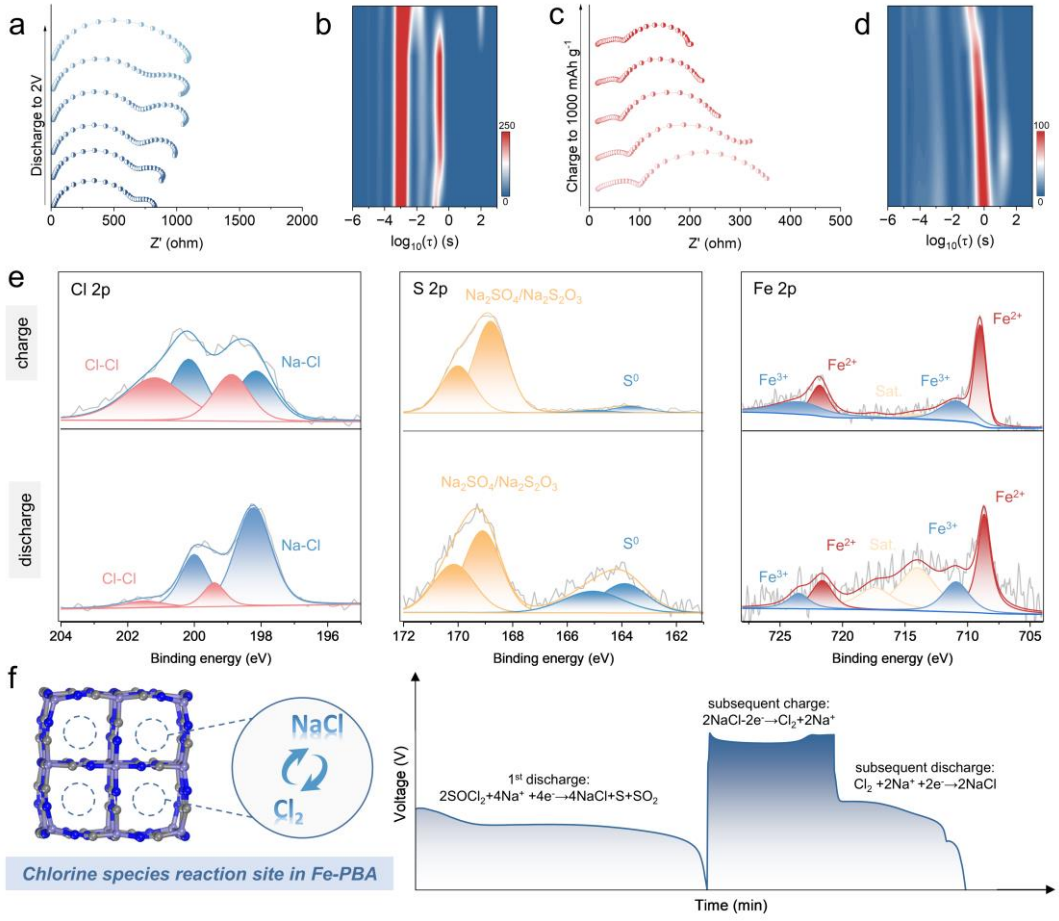

Figure 4. *(a) Ex situ EIS and (b) corresponding DRT spectra under different discharge states; (c) Ex situ EIS and (d) corresponding DRT spectra under different charge states; (e) XPS spectra of the cathode in charged and discharged states. (f) Schematic diagram of the working principle of Fe-PBA as cathode for Na-Cl_2 batteries.*

Based on the above analysis, the Fe-PBA open coordination framework can serve as an effective chlorine storage host in Na-Cl_2 batteries. Its three-dimensional open channels provide reaction space for chlorine-related species. The NaCl generated by the reduction of $SOCl_2$ during the first discharge can be deposited within the framework and reoxidized to release Cl_2 during subsequent charging cycles, enabling reversible conversion of chlorine species. As shown in Figure 4f, the initial discharge stage involves the reduction of $SOCl_2$ (Eq. (1)). After the initial charging, NaCl undergoes further oxidation to form Cl_2 (Eq. (2)), which is then reduced back to NaCl during discharge (Eq. (3)). The relevant chemical equations are as follows [1, 3]:

$$2SOCl_2+4Na^+ +4e^- \rightarrow 4NaCl+S+SO_2 \quad (1)$$

$$2NaCl-2e^- \rightarrow Cl_2+2Na^+ \quad (2)$$

$$Cl_2 +2Na^+ +2e^- \rightarrow 2NaCl \quad (3)$$

The Fe-PBA framework effectively supports the aforementioned reaction process by providing a stable open structure and storage space for chlorine species, thereby enabling a cyclable Na-Cl_2 electrochemical reaction. These results further demonstrate that Prussian blue analogs can serve as a new chlorine-storage cathode material, offering a new material option for the design of alkali metal-chlorine battery cathodes.

4. Conclusion

In this study, an iron-based Prussian blue analog open-framework cathode material was developed and successfully employed in Na-Cl_2 and Li-Cl_2 batteries. Fe-PBA features a typical monoclinic structure and a stable Fe-CN coordination network, providing effective storage space for chloride species and rapid ion transport pathways. In Na-Cl_2 batteries, Fe-PBA achieved more than 160 cycles of stable cycling at a capacity of 500mAh g^{-1} and retained a capacity of approximately 680mAh g^{-1} even under high-rate conditions of 3000 mA g^{-1}. Moreover, it exhibited excellent cycling stability and high-capacity output in Li-Cl_2 batteries as well, which demonstrates that Fe-PBA can facilitate the Cl_2/NaCl (LiCl) reversible conversion process. This work provides a new direction for the development of high-energy-density alkali-metal-chloride batteries.

Abbreviations

Fe-PBA	Prussian Blue Analogue
SEM	Scanning Electron Microscope
XRD	X-ray Diffraction
EIS	Electrochemical Impedance Spectroscopy
XPS	X-ray Photoelectron Spectroscopy

Author Contributions

Lina Ge: Conceptualization, Data curation, Resources, Visualization, Writing–original draft, Writing–review & editing

Yongpeng Cui: Conceptualization, Funding acquisition, Writing – review & editing

Wei Xing: Funding acquisition, Writing – review & editing

Funding

This work was supported by the National Natural Science Foundation of China (No. 22109178 and 52277229), the Beijing Nova Program (No. 20240484570), the Postdoctoral Fellowship Program of CPSF (No. GZB20240847), the Young Taishan Scholars Program of Shandong Province (No. tsqn202211082), the China Postdoctoral Science Foundation (No. 2024M753609), and the Fundamental Research Funds for the Central Universities (No. 25CX04001A and 2462023QNXZ015).

Data Availability Statement

The data is available from the corresponding author upon reasonable request.

Conflicts of Interest

The authors declare no conflicts of interest.

References

[1] G. Zhu, X. Tian, H.-C. Tai, Y.-Y. Li, J. Li, H. Sun, P. Liang, M. Angell, C.-L. Huang, C.-S. Ku, W.-H. Hung, S.-K. Jiang, Y. Meng, H. Chen, M.-C. Lin, B.-J. Hwang, H. Dai, Rechargeable Na/Cl_2 and Li/Cl_2 batteries, Nature. 596(2021) 525-530. http://doi.org/10.1038/s41586-021-03757-z

[2] P. Li, X. Li, Y. Guo, A. Chen, R. Zhang, Y. Hou, Q. Xiong, Y. Wang, Z. Chen, J. Zhu, M. Zhu, C. Zhi, Development of an energy-dense and high-power Li-Cl_2 battery using reversible interhalogen bonds, Chem. 10(2024) 352-364. http://doi.org/10.1016/j.chempr.2023.09.021

[3] P. Liang, G. Zhu, C. L. Huang, Y. Y. Li, H. Sun, B. Yuan, S. C. Wu, J. Li, F. Wang, B. J. Hwang, H. Dai, Rechargeable Li/Cl_2 battery down to -80 ℃, Adv. Mater. 36(2023) 2307192. http://doi.org/10.1002/adma.202307192

[4] P. Li, C. Ma, Y. Wang, S. Zhai, G.g Ma, D..Kong, Z. Li, Co single-atom catalysis for high-efficiency LiCl/Cl_2 conversion in rechargeable lithium-chlorine batteries, Adv. Mater. 37(2025) 2418990. http://doi.org/10.1002/adma.202418990

[5] Y. Xu, L. Jiao, J. Ma, P. Zhang, Y. Tang, L. Liu, Y. Liu, H. Ding, J. Sun, M. Wang, Z. Li, H.-L. Jiang, W. Chen, Metal-organic frameworks for nanoconfinement of chlorine in rechargeable lithium-chlorine batteries, Joule. 7(2023) 515-528. http://doi.org/10.1016/j.joule.2023.02.010

[6] G. Zhu, H. Xu, S. Wang, Y. Zhang, J.-H. Fang, T. Dai, D. J. Zheng, W. Chen, H. Roh, D. Wang, D. Menga, S. Yu, H. Iriawan, Y. Shao-Horn, J. Li, Increasingly reversible Na/Cl_2 and Li/Cl_2 batteries, J. Am. Chem. Soc. 148(2026) 22673-22686. http://doi.org/10.1021/jacs.6c02353

[7] G. Zhua, P. Liang, C. Huang, S. Wu, C. Huang, Y. Li, S. Jiang, W. H. Huang, J. Li, F. Wang, B. J. Hwang, H. Dai, Shedding light on rechargeable Na/Cl_2 battery, Proc. Natl. Acad. Sci. U. S. A. 120(2023) e2310903120. http://doi.org/10.1073/pnas

[8] P. Liang, G. Zhu, W. Wang, C.-L. Huang, S.-C. Wu, J. Zhou, X. Zhou, Y. Wu, S. Wang, M. Wang, L. Zhang, C. C. Ming, J. Li, F. Wang, M. Sun, Y.-Y. Li, B.-J. Hwang, H. Dai, Carbon nanotubes for rechargeable Na/Cl_2 batteries, J. Am. Chem. Soc. 147(2025) 18541-18549. http://doi.org/10.1021/jacs.4c18070

[9] Y. Xu, M. Wang, M. Sajid, Y. Meng, Z. Xie, L. Sun, J. Jin, W. Chen, S. Zhang, Organocatalytic lithium chloride oxidation by covalent organic frameworks for rechargeable lithium-chlorine batteries, Angew. Chem. Int. Ed. 63(2024) e202315931 http://doi.org/10.1002/anie.202315931

[10] K. J. Tuggle, E. E. Lane, A. H. Ellis, R. S. Arnold, W. D. McDearmon, H. M. Grace, B. J. McNicholas, Nonaqueous electrochemistry of prussian blue analogs: Synthesis, fundamental studies, and applications in battery chemistry, Coord. Chem. Rev. 548(2026) 217219. http://doi.org/10.1016/j.ccr.2025.217219

[11] C. Yang, Z. Chen, H. K. Liu, S. X. Dou, W. Huang, S. Chong, Prussian blue analogue cathodes for post-lithium-ion batteries: Recent advances and future perspectives, Adv. Energy Mater. 16(2026). http://doi.org/10.1002/aenm.70735

[12] Z. Jing, L. Kong, M. Mamoor, L. Wang, B. Zhang, B. Wang, Y. Zhai, F. Wang, G. Qu, Y. Kong, D. Wang, L. Xu, Rational design of prussian blue analogues for ultralong and wide-temperature-range sodium-ion batteries, J. Am. Chem. Soc. 147(2025) 3702-3713. http://doi.org/10.1021/jacs.4c16031

[13] J. Liu, Y. Wang, N. Jiang, B. Wen, C. Yang, Y. Liu, Vacancies-regulated prussian blue analogues through precipitation conversion for cathodes in sodium-ion batteries with energy densities over 500 wh/kg, Angew. Chem. Int. Ed. 63(2024) e202400214. http://doi.org/10.1002/anie.202400214

[14] L. Ge, Y. Song, P. Niu, B. Li, L. Zhou, W. Feng, C. Ma, X. Li, D. Kong, Z. Yan, Q. Xue, Y. Cui, W. Xing, Elaborating the crystal water of prussian blue for outstanding performance of sodium ion batteries, ACS Nano. 18(2024) 3542-3552. http://doi.org/10.1021/acsnano.3c11169

[15] W. Wang, Y. Gang, Z. Hu, Z. Yan, W. Li, Y. Li, Q. F. Gu, Z. Wang, S. L. Chou, H. K. Liu, S. X. Dou, Reversible structural evolution of sodium-rich rhombohedral prussian blue for sodium-ion batteries, Nat. Commun. 11(2020) 980. http://doi.org/10.1038/s41467-020-14444-4

[16] Y. Liu, Y. Qiao, W. Zhang, Z. Li, X. Ji, L. Miao, L. Yuan, X. Hu, Y. Huang, Sodium storage in Na-rich $Na_xFeFe(CN)_6$ nanocubes, Nano Energy. 12(2015) 386-393. http://doi.org/10.1016/j.nanoen.2015.01.012

[17] J. Liu, J. Liu, M. Tang, J. Fu, X. Kuang, J. Ma, Boosting sodium storage in prussian blue analogs through iron vacancies and copper doping, Adv. Funct. Mater. 34(2024) 2314167. http://doi.org/10.1002/adfm.202314167

[18] Y. Xu, S. Zhang, M. Wang, Y. Meng, Z. Xie, L. Sun, C. Huang, W. Chen, Enrichment of chlorine in porous organic nanocages for high-performance rechargeable lithium-chlorine batteries, J. Am. Chem. Soc. 145(2023) 27877-27885. http://doi.org/10.1021/jacs.3c11726

[19] W. Feng, X. Wei, J. Yang, C. Ma, Y. Sun, J. Han, D. Kong, L. Zhi, Iodine-induced self-depassivation strategy to improve reversible kinetics in Na-Cl_2 battery, Nat. Commun. 15(2024) 6904. http://doi.org/10.1038/s41467-024-51033-1

[20] X. Wei, D. Kong, W. Feng, F. Cao, C. Ma, J. Yang, J. Han, L. Wang, G. Ma, H. Wang, Y. Sun, Z. Liu, L. Wei, L. Zhi, Protonated pyridinic nitrogen enhances chloride conversion for ultrastable Li/Na-Cl_2 batteries, Adv. Energy Mater. 15(2025) 2501333. http://doi.org/10.1002/aenm.202501333

[21] W. Feng, J. Yang, X. Wei, C. Ma, J. Han, G. Ma, H. Wang, D. Kong, L. Zhi, Boosting ultra-wide temperature sodium-bromine batteries via chlorine-bromine activation, Angew. Chem. Int. Ed. 64(2025) e202503752. http://doi.org/10.1002/anie.202503752

[22] Y. Gao, X. Zhang, H. Zhang, J. Peng, W. Hua, Y. Xiao, X. H. Liu, L. Li, Y. Qiao, J. Z. Wang, C. Zhang, S. Chou, Zero-waste polyanion and prussian blue composites toward practical sodium-ion batteries, Adv. Mater. 37(2025) 2409782. http://doi.org/10.1002/adma.202409782